IEEE Access
Multidisciplinary | Rapid Review | Open Access Journal

Received November 2, 2019, accepted November 25, 2019, date of publication November 28, 2019,
date of current version December 12, 2019.

Digital Object Identifier 10.1109/ACCESS.2019.2956517

Laser Spatial Coherence Suppression With Refractive Optical Elements Toward the Improvement of Speckle Reduction by Light Pipes

ZHAOMIN TONG[1,2], CHANGYUAN SUN[1,2], YIFEI MA[1,2], MEI WANG[1,2], SUOTANG JIA[1,2], AND XUYUAN CHEN[1,2,3]

[1]State Key Laboratory of Quantum Optics and Quantum Optics Devices, Institute of Laser Spectroscopy, Shanxi University, Taiyuan 030006, China
[2]Collaborative Innovation Center of Extreme Optics, Shanxi University, Taiyuan 030006, China
[3]Department of Microsystems, University of South-Eastern Norway, 3184 Horten, Norway

Corresponding author: Zhaomin Tong (zhaomin.tong@sxu.edu.cn)

This work was supported in part by the National Key Research and Development Program of China under Grant 2016YFB0401903, in part by the Key Research and Development Program of Shanxi Province for International Cooperation under Grant 201703D421015, in part by the Changjiang Scholars and Innovative Research Team in University of Ministry of Education of China under Grant IRT_17R70, in part by the State Key Program of National Natural Science of China under Grant 11434007, in part by the 111 Project under Grant D18001, and in part by the Fund for Shanxi 1331 Project Key Subjects Construction.

ABSTRACT We study laser speckle reduction by light pipes, and we propose a new method to improve its efficiency. Proof-of-concept refractive optical elements (ROEs) with a staircase-like structure are introduced before a holographic diffuser to split a laser beam into laser sub-beams. Optical paths of the laser sub-beams after transmitting through the ROEs are different, and these partially correlated (or uncorrelated) laser sub-beams are added in intensity basis because of the folded mirror reflections by the light pipe. Thus, laser spatial coherence is suppressed, which helps to reduce speckle. We demonstrate this method in a simplified laser projection system, where subjective speckle contrast is reduced from 0.33 to 0.24 before and after introducing a two-dimensional ROE, respectively. Comparing with other improved speckle reduction methods by light pipes, the proposed method is motionless and simpler.

INDEX TERMS Speckle reduction, light pipe, refractive optical element.

I. INTRODUCTION

With the development of high-power and low-cost laser diodes (LDs), especially for green and red colors, laser display industry grows fast during the past years [1], [2]. The advantages of using LDs as illumination light sources in displays are obvious, for example, laser displays having wider color gamut and higher brightness [2]. But speckle, on the other hand, exists and is a problem in laser displays. In order to improve image quality, speckle reduction is required in laser displays. Speckle reduction can be realized by polarization diversity [3], [4], wavelength diversity [5], [6], and time-average of different speckle patterns [7]–[15], etc. However, these speckle reduction methods are either insufficient or cause tradeoffs. For example, polarization diversity can only reduce speckle by $1/4^{1/2}$, where depolarization of the projection screen can provide the first two degrees of speckle reduction freedom [3], and the other two degrees of speckle reduction freedom can be obtained by rotating the polarization orientation of LDs [4]; wavelength diversity is constrained by the choice of LD wavelengths. Currently, LD modules with six-primary or nine-primary wavelengths can be achieved by using LDs with different wavelengths purchased from Nichia and Necsel [16], [17]. LD modules with more primary wavelengths require the customizations of laser design and fabrication, which are costly; time-average of different speckle patterns is commonly used and is efficient for speckle reduction. For example, dynamic diffractive optical elements (DOEs) made of polydimethylsiloxane are used for speckle reduction [15]. The dynamic DOEs

The associate editor coordinating the review of this manuscript and approving it for publication was Chao Zuo.

employ switchable diffraction gratings to generate different speckle patterns, where independent controlling electrodes are required for driving the diffraction gratings. The problem for speckle reduction achieved by time-average of different speckle patterns is that actuators or motors are required to drive the device, which are normally noisy and increase the complexity of the projection system.

Light pipes are essential optical devices in projection displays to homogenize light [18]. Besides this function, we find that with the enhancement of the modal dispersion among the guided wave modes by increasing the working numerical aperture and/or the length of a light pipe, laser speckle at the exit facet of the light pipe can be reduced. Similar speckle reduction mechanism employed in another kind of optical waveguide: a step-index optical fiber has been well studied [19], [20]. In [19], the authors investigated the conditions to achieve speckle contrast ratio equaling to 0.01 at the exit facet of the multimode fiber, where the light source was a LD having a Gaussian spectral profile with 1/*e* half wavelength of 1 nm; as an example, the required length of the multimode fiber was 5 m when the numerical aperture of the multimode fiber was 0.8 [19]. The same level of speckle contrast ratio at the exit facet of light pipes is unachievable, because the length of light pipes in projection displays typically ranges from tens to hundreds millimeters, *i.e.*, the length of light pipes is too short. In order to further reduce speckle, placing a changing diffuser before light pipes and vibrating or rotating light pipes have been used [21]–[24]. However, these time-averaging methods have the tradeoffs as we have explained above.

In this paper, we study speckle reduction by light pipes, and we propose a motionless and simple method to improve its efficiency. The main contents of the paper are organized as follows: firstly, holographic diffusers with different diffusing angles θ_d are used to simulate the influence of the working numerical aperture of the light pipe on objective speckle reduction, and we investigate objective speckle reduction by employing light pipes with different lengths L_{LP}. Secondly, by assembling glasses with different heights, three kinds of proof-of-concept refractive optical elements (ROEs) with a staircase-like structure are fabricated, namely one-dimensional ROE aligned in the horizontal direction ($\mathrm{ROE_{1DH}}$), one-dimensional ROE aligned in the vertical direction ($\mathrm{ROE_{1DV}}$) and two-dimensional ROE ($\mathrm{ROE_{2D}}$). We place the ROEs before the holographic diffuser, and the diameter of a laser beam is adjusted to make the change of the number of laser sub-beams divided by the ROEs. Thus, after capturing objective speckles formed on a sandblasted glass diffuser which is placed closely after the exit facet of the light pipe, the improvement of objective speckle reduction with the helps of the ROEs is studied. Thirdly, we demonstrate the improvement of subjective speckle reduction with the help of the $\mathrm{ROE_{2D}}$ in a simplified projection system. Comparing with the time-averaging methods, the method presented in this paper is motionless and simpler, making it more suitable for speckle reduction application in laser displays.

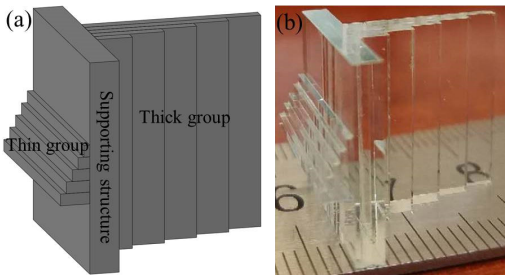

FIGURE 1. The proof-of-concept ROEs with the staircase-like structure are fabricated by assembling glasses. The schematic (a) and the real image (b) of the ROEs.

II. DEVICE FABRICATION AND EXPERIMENTAL SETUP

The proof-of-concept ROEs with the staircase-like structure are fabricated by assembling glasses. Figure 1 shows the schematic and the real image of the fabricated ROEs. A piece of glass is cut into two groups of glasses, where the individual glass has the same length of 18 mm and the same width of 1 mm. The heights of these two groups of glasses are different, varying from 0.5 mm to 2.5 mm with an even increment of $\Delta d_{\mathrm{1DH}} = 0.5$ mm and from 3 mm to 15 mm with an even increment of $\Delta d_{\mathrm{1DV}} = 3$ mm, respectively. Sidewalls of the glasses are polished using grinding process. As shown in Figure 1, the thin and thick groups of glasses are assembled by gluing with UV resin in the horizontal and vertical directions, respectively, where an 18 mm $\times$ 18 mm $\times$ 2.5 mm glass substrate works as the supporting structure in between them.

Figure 2(a) schematically shows the experimental setup for objective speckle measurements, and Figure 2(b) illustrates the relationship among the dimensions of the $\mathrm{ROE_{2D}}$ (square region in dark gray color, 6 mm $\times$ 6 mm), the diameter of an exampled aperture of the iris D_{iris} (circular region within the red line), and the entrance facet of the tapered light pipe (square region in green color, 4 mm $\times$ 4 mm). As shown in Figure 2(a), a collimated laser beam generated from a LD (L520P50 from Thorlabs) with a multiline spectrum and the central wavelength at $\lambda_c = 520$ nm is expanded as a 30 mm in diameter circular laser beam by a beam expander. The driving current of the LD is 150 mA, and the working temperature of the LD is maintained at 20°C using a thermoelectrically cooled mount. An iris with laser-engraved scales (SM1D12C from Thorlabs, the diameter of the circular aperture varies from $D_{iris} = 1$ mm to $D_{iris} = 12$ mm) is placed after the expanded laser beam to redefine the laser beam diameter. In laser projection displays, a weak-scattering holographic diffuser is usually employed to improve the homogenizing effect of light pipes by placing it closely before the entrance facet of light pipes [20]. In our experiments, the ROEs are placed before the holographic diffuser, followed by a tapered light pipe. A sandblasted glass diffuser is placed closely after the exit facet of the tapered light pipe, and objective speckles formed on the sandblasted glass diffuser are captured by a charge-coupled device (CCD) camera. In order to correctly capture speckle images, the exposure time of the CCD camera

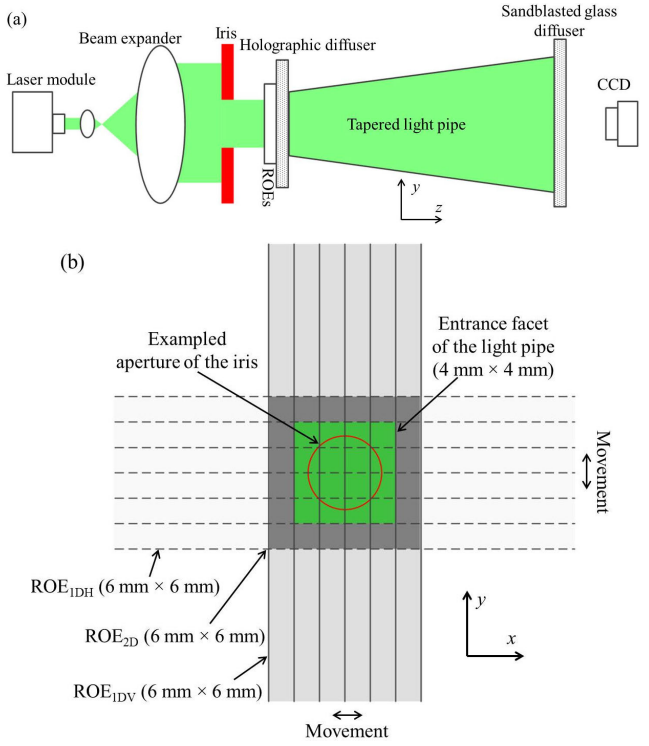

FIGURE 2. Schematic of experimental setup for objective speckle measurement (a) and the relationship among the dimensions of the ROE_{2D}, the diameter of an exampled aperture of the iris, and the entrance facet of the tapered light pipe (b).

TABLE 1. Dimensions of the tapered light pipes.

Length: L_{LP} (mm)	Width and height of entrance facet (mm)	Width and height of exit facet (mm)
50	4 × 4	8 × 8
100	4 × 4	8 × 8
140	4 × 4	8 × 5

is adjusted to make the CCD sensors working in their linear region. The distance from the sandblasted glass diffuser to the CCD camera is 600 mm.

Table 1 lists the dimensions of the three types of tapered light pipe used in our experiments, where they are categorized by the length of the tapered light pipe L_{LP}. The entrance facets of these light pipes have the same widths and heights of 4 mm × 4 mm. From Figure 2(b), we can find that when the diameter of the aperture of the iris equals to $D_{iris} \approx 6$ mm, the redefined laser beam can cover the whole entrance facet of the light pipe. In our experiments, we adjust the diameter of the aperture of the iris varying from $D_{iris} = 1$ mm to $D_{iris} = 6$ mm to study the speckle reduction efficiency. The ROEs are moved horizontally and vertically, thus, the overlapping region of the ROEs with the aperture of the iris and the entrance facet of the light pipe changes, and we can obtain speckle reduction with the helps of the ROE_{1DH} ($\Delta d_{1DH} = 0.5$ mm), ROE_{1DV} ($\Delta d_{1DV} = 3$ mm) and ROE_{2D} ($\Delta d_{2D} = 0.5$ mm).

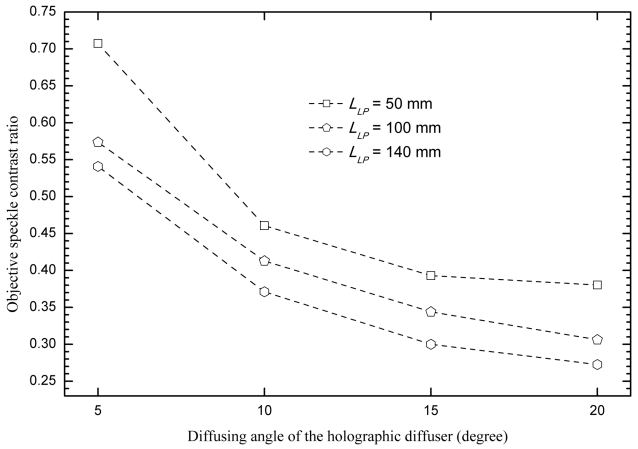

FIGURE 3. Relationship between the diffusing angle of the holographic diffuser θ_d and the objective speckle contrast ratio C.

III. EXPERIMENTAL RESULTS AND DISCUSSIONS

A. SPECKLE REDUCTION BY LIGHT PIPES

By using the optical setup shown in Figure 2(a) after removing the ROEs, Figure 3 presents the experimental results about the relationship between the diffusing angle of the holographic diffuser θ_d and the objective speckle contrast ratio C. The three types of tapered light pipes listed in Table 1 are employed to investigate the effect of the change of the length of light pipes L_{LP} on speckle reduction. We have used holographic diffusers with diffusing angles θ_d of 5°, 10°, 15° and 20° (full width at half maximum). The diameter of the iris aperture has a constant value of $D_{iris} = 1$ mm.

From Figure 3, we can find that with the increase of the diffusing angle of the holographic diffuser θ_d, objective speckle contrast ratio C decreases for the three types of tapered light pipe; it can also be found that light pipes with longer lengths reduce speckle more efficiently than the shorter ones at the same diffusing angle of the holographic diffuser θ_d. These observations can be explained in consideration of the modal dispersion in another kind of optical waveguide: a step-index multimode fiber [19]. For the step-index multimode fiber, the temporal pulse spreading $\delta\tau$ caused by the modal dispersion equals to:

$$\delta\tau = \frac{L_{MMF}\,(NA)^2_{MMF}}{2n_{core}c} \tag{1}$$

where L_{MMF}, NA_{MMF} and n_{core} represent the length, numerical aperture and refractive index of the core of the step-index multimode fiber, respectively, and c is the speed of light in vacuum [19]. Consider a LD having a multiline spectrum, where the individual lines in the spectrum have Gaussian profiles with 1/e half widths of $\Delta\lambda$, the center-to-center spacing between the lines equals to $\Delta\lambda_s$, and the LD spectrum is modulated by a Gaussian envelop function with a 1/e half width of $\Delta\lambda_e$, laser beam generated by the LD is coupled into the step-index multimode fiber. The square of speckle contrast ratio C_{MMF} at the exit facet of the step-index

multimode fiber can be written as [19], [25]

$$C_{MMF}^2 = \psi_1^{-1/2} \frac{\sum_m \sum_n \psi_2 \exp\left\{-\left[\frac{(m-n)\Delta\lambda_s}{2^{1/2}\Delta\lambda}\right]^2 \left(1-\psi_1^{-1}\right)\right\}}{\sum_m \sum_n \psi_2} \tag{2}$$

where

$$\psi_1 = \left[1 + \frac{1}{2}\left(2\pi c \frac{\delta\tau\,\Delta\lambda}{\sqrt{3}\lambda^2}\right)^2\right]$$
$$\psi_2 = \exp\left\{-\left[\frac{\left(m^2+n^2\right)\Delta\lambda_s^2}{\Delta\lambda_e^2}\right]\right\} \tag{3}$$

and m and n represents the mth and nth spectrum lines of the LD, respectively.

According to (2) and (3), the square of speckle contrast ratio C_{MMF} at the exit facet of the step-index multimode fiber is inversely proportional to the temporal pulse spreading $\delta\tau$. Thus, one can suppress speckle by increasing the temporal pulse spreading $\delta\tau$, *i.e.*, by increasing the length L_{MMF} and/or numerical aperture NA_{MMF} of the step-index multimode fiber based on (1) [19].

Light pipes are similar optical waveguides with step-index multimode fibers, where speckles form because of the interferences of the guided waves that travel along different optical paths due to multiple reflections and add up in phase basis. There are three speckle formation mechanisms in Figure 2(a), *i.e.*, speckles caused by the holographic diffuser, the tapered light pipe and the sandblasted glass diffuser. The objective speckle contrast ratios C shown in Figure 3 are the compounded values caused by these three factors. Because the holographic diffuser and the sandblasted glass diffuser are static, they have no contributions to speckle reduction; speckle reduction is attributed to the increase of the temporal pulse spreading $\delta\tau$ of the tapered light pipe. When the diffusing angle of the holographic diffuser θ_d, *i.e.*, the working numerical aperture of the taped light pipe and the length of the taped light pipe L_{LP}, are increased, the temporal pulse spreading $\delta\tau$ caused by the modal dispersion in the tapered light pipe increases, and consequentially, speckle is reduced referring to (1) and (2) for the step-index multimode fiber.

$\sim 20\%$ optical power is found to be lost after introducing the ROEs. This is mainly because of the reflections occurring between air and glass interfaces and the defects introduced by the UV resin during the glass assembling process. By using antireflection coatings and improving the glass assembling process, the optical power loss after introducing the ROEs can be minimized. During the experiment, additional optical power loss is observed when the diffusing angle of the holographic diffuser θ_d increases. The critical angle of the tapered light pipes is $180 \times \sin^{-1}(1/n_{LP}) / \pi = 180 \times \sin^{-1}(1/1.52) / \pi \approx 41°$, where the light pipes are made of N-BK7 whose refractive index equals to $n_{LP} = 1.52$ at $\lambda_c = 520$ nm wavelength. Though the total internal reflection condition for the guided lights inside the tapered light pipe is always satisfied, more lights are reflected at the entrance facet of the tapered light pipe (the air/N-BK7 interface) when the diffusing angle of the holographic diffusers θ_d increases according to the Fresnel equations [26].

If we replacing the ROEs in Figure 2(a) by static DOEs, lower objective speckle CRs are expected to be obtained comparing with the experimental results presented in Figure 3 (without ROEs or DOEs). This is because the working numerical aperture of the taped light pipe is increased by the DOEs, which in turn increases the modal dispersion in the tapered light pipe and reduces speckle. However, one should know that additional optical power loss will be caused by the DOEs because of the diffracted laser beam. ROEs, on the contrary, have no such problem, where the laser beam quality is maintained.

B. IMPROVEMENT OF SPECKLE REDUCTION USING THE ROEs

Our first step is to demonstrate and compare the improvements of speckle reduction by the $\text{ROE}_{1\text{DH}}$ ($\Delta d_{1DH} = 0.5$ mm), $\text{ROE}_{1\text{DV}}$ ($\Delta d_{1DV} = 3$ mm) and $\text{ROE}_{2\text{D}}$ ($\Delta d_{2D} = 0.5$ mm) for the same holographic diffuser with a $\theta_d = 5°$ diffusing angle and the same $L_{LP} = 50$ mm long tapered light pipe. Figure 4 shows the objective speckle contrast ratio C and the equivalent number of independent speckle patterns N_{exp} when the diameter of the aperture of the iris D_{iris} changes, where we have also conducted experiments without the ROEs for comparison. The value of N_{exp} is obtained by

$$N_{\text{exp}} = \left(C_0 / C_{ROE}\right)^2 \tag{4}$$

where C_0 and C_{ROE} represent objective speckle contrast ratios without and with the ROEs, respectively. The reason that we introduce the equivalent number of independent speckle patterns N_{exp} is to compare this value with the equivalent number of independent laser sub-beams N_{theory} determined by the number of ROE cells inside the working area of the ROEs (*i.e.*, the diameter of the aperture of the iris).

From Figure 4, we can find that the objective speckle contrast ratio decrease with the increase of the diameter of the aperture of the iris D_{iris}. For the condition without using the ROEs (hollow square-dash line), this trend can be explained by the influence of the working numerical aperture of the tapered light pipe on the temporal pulse spreading $\delta\tau$ and the speckle contrast ratio using (1) to (3). In cases after introducing the $\text{ROE}_{1\text{DH}}$ (hollow up triangle-solid line), $\text{ROE}_{1\text{DV}}$ (hollow down triangle-solid line) and $\text{ROE}_{2\text{D}}$ (hollow square-solid line), the spatial coherence of the LD is destroyed because the temporal coherence of the LD is suppressed after bringing optical path differences among the laser sub-beams defined by the ROE cells [3]; a larger value of D_{iris} introduce more laser spatial coherence suppression, and hence the objective speckle contrast ratio decreases with the increase of the diameter of the aperture of the iris D_{iris}.

It can also be found from Figure 4 that for a constant value of D_{iris}, the speckle contrast ratio when using the $\text{ROE}_{1\text{DV}}$ (hollow down triangle-solid line) is lower than that when

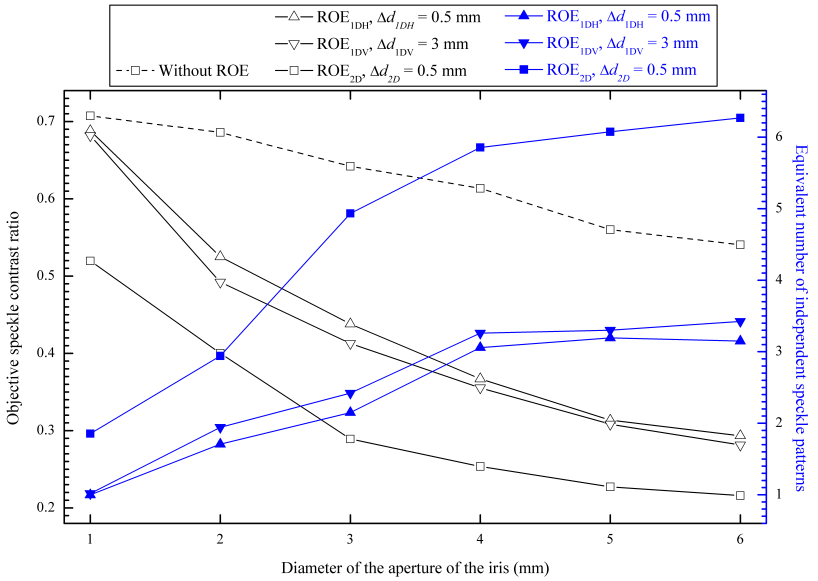

FIGURE 4. Objective speckle contrast ratio C and equivalent number of independent speckle patterns N_{exp} with the change of the diameter of the aperture of the iris by introducing the ROE_{1DH}(Δd_{1DH} = 0.5mm), ROE_{1DV} (Δd_{1DV} = 3mm) and ROE_{2D}(Δd_{2D} = 0.5 mm). We have also conducted experiment without using the ROEs for comparison. The holographic diffuser has a diffusing angle of $\theta_d = 5°$, and the length of the tapered light pipe is L_{LP} = 50 mm.

using the ROE_{1DH} (hollow up triangle-solid line), and the lowest speckle contrast ratio is obtained after introducing the ROE_{2D} (hollow square-solid line). The multiline spectrum of the LD is measured by a spectrometer (Aryelle Butterfly bought from LTB), and we find that the Gaussian envelop function modulating the spectrum has a 1/e half width of $\Delta\lambda_e = 0.77$ nm. The coherence length of the LD L_c can be calculated as $L_c \approx \lambda_c^2 / \Delta\lambda_e = 520^2 / 0.77 = 3.5 \times 10^5$ nm [27]. Consider the height difference of two adjacent ROE_{1DH} cells is $\Delta d = 0.5$ mm, and the ROE_{1DH} is made of fused silica with the refractive index of $n_{ROE} = 1.46$ at 520 nm, the optical path difference caused by two adjacent ROE_{1DH} cells is $\Delta d_{OPD\_1DH} = \Delta d_{1DH} \times (n_{ROE} - n_{air}) = 0.5 \times (1.46 - 1) = 0.23$ mm, where n_{air} is the refractive index of air. Because $\Delta d_{OPD\_1DH} < L_c$, the laser sub-beams defined by the ROE_{1DH} cells is partially correlated; when the ROE_{1DV} is used, the optical path difference caused by two adjacent ROE_{1DV} cells is calculated as $\Delta d_{OPD\_1DV} = 1.38$ mm, which is larger than L_c, which means that the ROE_{1DV}, in principle, can fully destroy the spatial coherence of the LD [3]. Therefore, the introduction of ROE_{1DV} is more efficient than ROE_{1DH} for the improvement of speckle reduction by light pipes, *i.e.*, we can obtain lower speckle contrast ratio when using the ROE_{1DV} than the ROE_{1DH} as shown in Figure 4. As for the reason that the lowest speckle contrast ratios are achieved by using the ROE_{2D} in comparisons with the introductions of the ROE_{1DH} and ROE_{1DV} in Figure 4, it is straightforward because more numbers of ROE cells that generate partially correlated laser sub-beams are introduced when using the two-dimension ROE: ROE_{2D} than the one-dimensional ROEs: ROE_{1DH} and ROE_{1DV}.

In Figure 4, one can see that the equivalent number of independent speckle patterns N_{exp} (solid up triangle-solid line, solid down triangle-solid line and solid square-solid line) increase when the aperture of the iris becomes larger. This is because the equivalent number of independent laser sub-beams N_{theory} changes with the aperture of the iris. Calculation of N_{theory} can be achieved by using the following procedure. For example, consider the introduction of the ROE_{1DV}, Figure 5 schematically presents the relationship among the dimensions of the ROE_{1DV} (6 mm × 6mm), the aperture of the iris D_{iris} and the entrance facet of the light pipe (4 mm × 4 mm).

As shown in Figure 5, when the aperture of the iris D_{iris} is adjusted, the values of the areas of the laser sub-beams (A_{-2}, A_{-1}, A_0, A_1 and A_2) defined by the ROE_{1DV} cells vary, which results in the change of the ratio among them. Table 2 lists the normalized value of the area of the laser sub-beam A, the equivalent number of independent laser sub-beams N_{theory}, and the equivalent number of independent speckle patterns N_{exp} obtained from Figure 4. The equivalent number of independent laser sub-beams N_{theory} is calculated by the assumption of summing M independent speckle patterns with different mean intensity $\bar{I}$, such as [28]

$$C_s = \left(\sum_{m=1}^{M} \overline{I_m}^2\right)^{1/2} \Big/ \sum_{m=1}^{M} \overline{I_m} \tag{5}$$

$$N_{theory} = 1 \Big/ C_s^2 \tag{6}$$

where the individual speckle patterns have a speckle contrast ratio equaling to one, and C_s and $\overline{I_m}$ represent speckle contrast for the summed speckle image and the mean intensity of

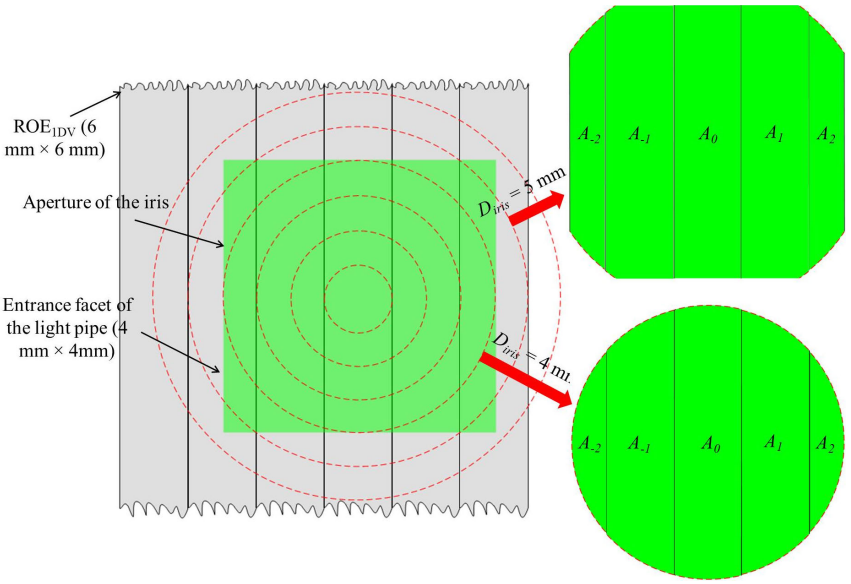

FIGURE 5. Schematic of the relationship among the dimensions of the ROE_{1DV} (6 mm × 6mm), the aperture of the iris D_{iris}, and the entrance facet of the light pipe (4 mm × 4mm). The aperture of the iris varies from $D_{iris} = 1$ mm to $D_{iris} = 6$ mm. In the figure, we present two examples about the obtained laser sub-beams are presented when $D_{iris} = 4$ mm and $D_{iris} = 5$ mm, where the laser beam is divided into five laser sub-beams with the values of areas equaling to A_{-2}, A_{-1}, A_0, A_1 and A_2.

the mth speckle pattern, respectively. It is obvious that C_s is influenced by the ratio among the mean intensities of the individual speckle patterns according to (5). Because the mean intensity of the mth individual speckle pattern $\overline{I_m}$ is determined by the area of the mth laser sub-beam A_m, and the laser beam emitted from the LD is expanded uniformly, we can rewrite (5) into

$$C_s = \left(\sum_{m=1}^{M} A_m^2\right)^{1/2} \Big/ \sum_{m=1}^{M} A_m \tag{7}$$

Therefore, the equivalent number of independent laser sub-beams N_{theory} can be obtained from (6) and (7) after knowing the normalized value of the area of the laser sub-beam A.

From table 2, we can find that N_{theory} increases significantly when D_{iris} is changed from $D_{iris} = 1$ mm to $D_{iris} = 4$ mm, and the increase rate of N_{theory} becomes slower from $D_{iris} = 4$ mm to $D_{iris} = 6$ mm. Comparing with the change of the equivalent number of independent speckle patterns N_{exp} when D_{iris} is increased for the ROE_{1DV} presented in Figure 4 (solid down triangle-solid line), the trend obtained experimentally is consistant with theoritical expection. In table 2, we can also find that the value of N_{exp} is lower than that of N_{theory} for the same D_{iris} ranging from $D_{iris} = 2$ mm to $D_{iris} = 6$ mm. This is because in the procedure of calculating N_{theory}, we have assumed that the M speckle patterns are independent. However, because the speckle reduction mechanisms by introducing light pipes and ROEs are similar (correlated), *i.e.*, both by suppressing the spatial coherence of the LD using the reduction of the temporal coherence of the LD [3], where the modal dispersion and the staircase-like structure introduce temporal pulse spreading (optical path difference) in light pipes and ROEs, respectively, the validity of this assumption is not held, especially when the speckle reduction mechanism by light pipes becomes more dominate.

TABLE 2. Lists of the normalized value of the area of the laser sub-beam: A, the equivalent number of independent laser sub-beams: N_{theory} based on (6) and (7) and the equivalent number of independent speckle patterns: N_{exp} obtained from Figure 4. The ROE used here is ROE_{1DV}.

Diameter of the aperture of the iris: D_{iris} (mm)	A						
	A_{-2}	A_{-1}	A_0	A_1	A_2	N_{theory}	N_{exp}
1	0	0	1	0	0	1	1.02
2	0	0.32	1	0.32	0	2.23	1.94
3	0	0.7	1	0.7	0	2.91	2.42
4	0.23	0.86	1	0.86	0.23	3.91	3.26
5	0.44	1	1	1	0.44	4.44	3.3
6	0.5	1	1	1	0.5	4.57	3.42

The degeneration of the speckle reduction efficiency using the ROEs because of the correlated light pipes can be further explained by increasing the working numerical aperture (the diffusing angle of the holographic diffuser θ_d) and length of the light pipe L_{LP}, *i.e.*, by enhancing the speckle reduction mechanism by light pipes. Figure 6 shows these degenerations, where the ROE_{2D} is used.

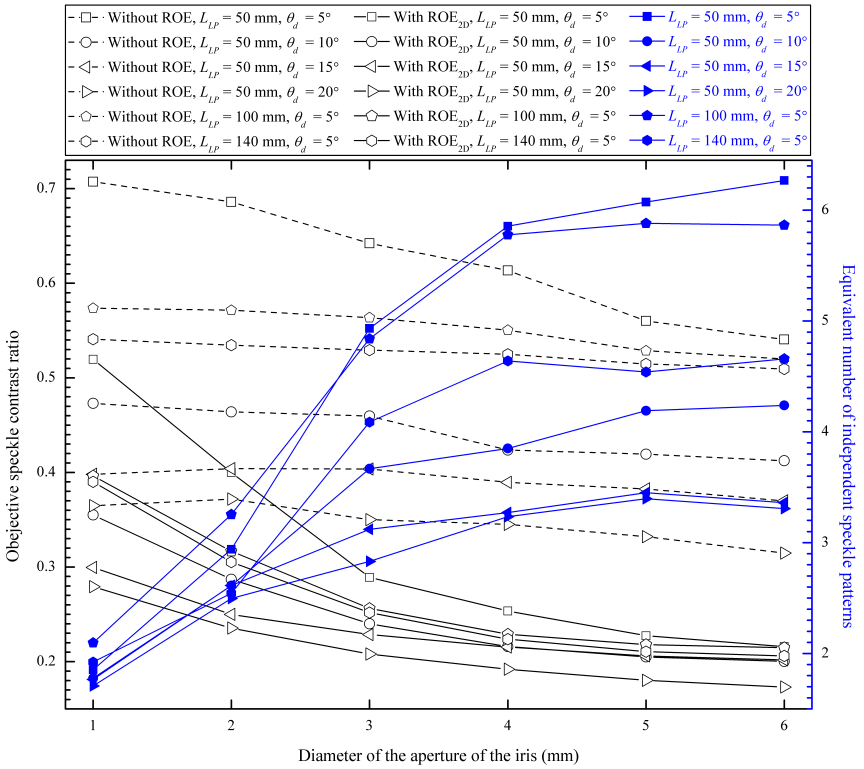

FIGURE 6. Objective speckle contrast ratio C and equivalent number of independent speckle patterns N_{exp} with the change of the diameter of the aperture of the iris by introducing the ROE$_{2D}$, where the diffusing angle of the holographic diffuser θ_d and the length of the tapered light pipe L_{LP} are changed. We can find that the speckle reduction efficiency using the ROE$_{2D}$ degenerates when the effect of light pipe on speckle reduction is enhanced by increasing θ_d and L_{LP}.

As shown in Figure 6, at a constant diameter of the aperture of the iris D_{iris}, the largest value of N_{exp} is almost always obtained when the smallest diffusing angle of the holographic diffuser $\theta_d = 5°$ and the shortest length of the light pipe $L_{LP} = 50$ mm are used (solid square-solid line); while, the combination of the largest diffusing angle of the holographic diffuser $\theta_d = 20°$ and $L_{LP} = 50$ mm provides the lowest value of N_{exp} (solid right triangle-solid line). From Figure 6, we can also find that by using the same holographic diffuser with a diffusing angle of $\theta_d = 5°$, the lowest value of N_{exp} corresponds to the condition when $L_{LP} = 140$ mm at a constant diameter of the aperture of the iris D_{iris} (solid hexagon-solid line). Based on these experimental results, it is clear that the improvement of speckle reduction with the helps of ROEs is affected by the parameters of the light pipe (working numerical aperture and length).

C. DEMONSTRATION OF THE IMPROVEMENT OF SPECKLE REDUCTION USING THE ROE2D IN A SIMPLIFIED LASER PROJECTION SYSTEM

For the demonstration of the method in a simplified projection system, Figure 2(a) is modified by removing the sandblasted glass diffuser, and we put a transparent glass with a stamped Chinese character closely after the exit facet of the light pipe. A focal length of $f_p = 60$ mm and F-number of $F\#_p = 5.6$ projection lens magnifies the Chinese character onto a painted white screen. The distance from the projection lens to the painted white screen is $Z_p = 240$ mm. Subjective speckles formed on the painted white screen are captured by the CCD

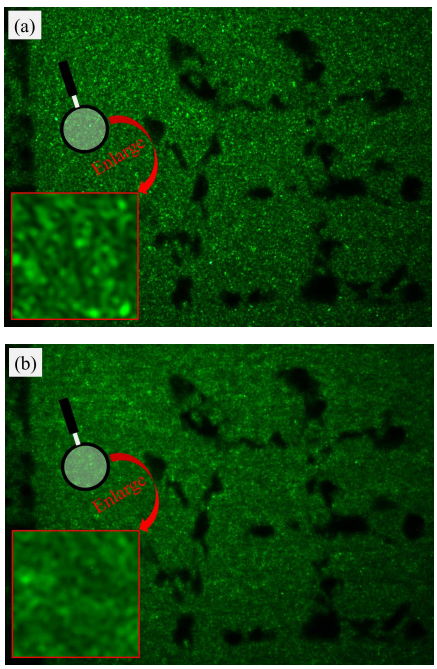

FIGURE 7. Subjective speckle images before (a) and after (b) introducing the ROE$_{2D}$ in a simplified laser projection system. The diameter of the aperture of the iris is $D_{iris} = 6$ mm, the diffusing angle of the holographic diffuser is $\theta_d = 5°$, and length of the light pipe is $L_{LP} = 140$ mm.

camera mounted with an imaging lens. The focal length of the imaging lens is $f_i = 35$ mm, and the F-number of the imaging lens has a constant value of $F\#_i = 22$. The distance from the imaging lens to the painted white screen is $Z_i = 120$ mm. Figure 7 shows the projected images before and after introducing the two-dimensional ROE: $\mathrm{ROE_{2D}}$, where $D_{iris} = 6$ mm, $\theta_d = 5°$ and $L_{LP} = 140$ mm.

Subjective speckle contrast ratios are calculated by choosing the uniform illuminated areas in Figure 7 (the enlarged areas), which are $C_{before} = 0.33$ and $C_{after} = 0.24$ before and after introducing the $\mathrm{ROE_{2D}}$, respectively.

IV. CONCLUSION

In this study, we have investigated speckle reduction by light pipes, and we have introduced the ROEs to improve its efficiency. The proof-of-concept ROEs were fabricated by assembling polished glasses with different thickness. After introducing the ROEs, a laser beam was divided as partially correlated (or uncorrelated) laser sub-beams, and the light pipe added up the speckle fields generated from the laser sub-beams in intensity basis. We have studied speckle reductions under different experimental conditions. We found that the efficiency of the improvement of speckle reduction by light pipes using the ROEs degenerated when the working numerical aperture and the length of the light pipe were increased. The proposed method was demonstrated in a simplified laser projection system, where its feasibility was verified. The speckle reduction method presented in this paper is motionless and simpler, making it superior to other methods such as by time-averaging different speckle patterns. In future, we plan to fabricate ROEs with smaller cell dimensions by using microfabrication process; thus, we can divide a laser beam into more numbers of partially correlated (or uncorrelated) laser sub-beams, and the efficiency of the improvement of speckle reduction by light pipes using the ROEs is expected to be optimized.

REFERENCES

[1] M. Murayama, Y. Nakayama, K. Yamazaki, Y. Hoshina, H. Watanabe, N. Fuutagawa, H. Kawanishi, T. Uemura, and H. Narui, "Watt-class green (530 nm) and blue (465 nm) laser diodes," *Phys. Status Solidi A*, vol. 215, May 2018, Art. no. 1700513.

[2] K. V. Chellappan, E. Erden, and H. Urey, "Laser-based displays: A review," *Appl. Opt.*, vol. 49, no. 25, pp. F79–F98, 2010.

[3] J. Goodman, "Speckle in optical projection displays," in *Speckle Phenomena in Optics: Theory and Applications*. Englewood, CO, USA: Roberts and Company Publishers, 2006, pp. 203–228.

[4] Z. Tong and X. Chen, "Speckle contrast for superposed speckle patterns created by rotating the orientation of laser polarization," *J. Opt. Soc. Amer. A*, vol. 29, no. 10, pp. 2074–2079, 2012.

[5] A. Furukawa, N. Ohse, Y. Sato, D. Imanishi, K. Wakabayashi, S. Ito, K. Tamamura, and S. Hirata, "Effective speckle reduction in laser projection displays," *Proc. SPIE*, vol. 6911, Jan. 2008, Art. no. 69110T.

[6] D. V. Kuksenkov, R. V. Roussev, S. Li, W. A. Wood, and C. M. Lynn, "Multiple-wavelength synthetic green laser source for speckle reduction," *Proc. SPIE*, vol. 7917, Feb. 2011, Art. no. 79170B.

[7] J. I. Trisnadi, "Hadamard speckle contrast reduction," *Opt. Lett.*, vol. 29, no. 1, pp. 11–13, 2004.

[8] M. N. Akram, Z. Tong, G. Ouyang, X. Chen, and V. Kartashov, "Laser speckle reduction due to spatial and angular diversity introduced by fast scanning micromirror," *Appl. Opt.*, vol. 49, no. 17, pp. 3297–3304, 2010.

[9] S. Kubota and J. W. Goodman, "Very efficient speckle contrast reduction realized by moving diffuser device," *Appl. Opt.*, vol. 49, no. 23, pp. 4385–4391, 2010.

[10] J.-Y. Lee, T.-H. Kim, B. Yim, J.-U. Bu, and Y.-J. Kim, "Speckle reduction in laser picoprojector by combining optical phase matrix with twin green lasers and oscillating MEMS mirror for coherence suppression," *Jpn. J. Appl. Phys*, vol. 55, no. 8S3, 2016, Art. no. 08RF03.

[11] Z. Tong, W. Shen, S. Song, W. Cheng, Z. Cai, Y. Ma, L. Wei, W. Ma, L. Xiao, S. Jia, and X. Chen, "Combination of micro-scanning mirrors and multi-mode fibers for speckle reduction in high lumen laser projector applications," *Opt. Express*, vol. 25, no. 4, pp. 3795–3804, 2017.

[12] J.-W. Pan and C.-H. Shih, "Speckle noise reduction in the laser mini-projector by vibrating diffuser," *J. Opt.*, vol. 19, no. 4, 2017, Art. no. 045606.

[13] H.-A. Chen, J.-W. Pan, and Z.-P. Yang, "Speckle reduction using deformable mirrors with diffusers in a laser pico-projector," *Opt. Express*, vol. 25, no. 15, pp. 18140–18151, 2017.

[14] Z. Tong, W. Cheng, S. Jia, and X. Chen, "Weak-scattering static diffuser by fast pumping dispersed-nanoparticles in a long distance using microfluidic flows for efficient laser speckle reduction," *Opt. Express*, vol. 26, no. 16, pp. 20270–20280, 2018.

[15] G. Ouyang, Z. Tong, M. N. Akram, K. Wang, V. Kartashov, X. Yan, and X. Chen, "Speckle reduction using a motionless diffractive optical element," *Opt. Lett*, vol. 35, no. 17, pp. 2852–2854, 2010.

[16] *Laser Diode*. Accessed: Oct. 9, 2019. [Online]. Available: https://www.nichia.co.jp/en/product/laser.html

[17] *Laser*. Accessed: Oct. 9, 2019. [Online]. Available: https://www.ushio.com/lasers

[18] M. Brennesholtz and E. Stupp, "Integrators," in *Projection Displays*. Hoboken, NJ, USA: Wiley, 2008, pp. 96–105.

[19] J. G. Manni and J. W. Goodman, "Versatile method for achieving 1% speckle contrast in large-venue laser projection displays using a stationary multimode optical fiber," *Opt. Express*, vol. 20, no. 10, pp. 11288–11315, 2012.

[20] A. Efimov, "Coherence and speckle contrast at the output of a stationary multimode optical fiber," *Opt. Lett.*, vol. 43, no. 19, pp. 4767–4770, 2018.

[21] J.-W. Pan and C.-H. Shih, "Speckle reduction and maintaining contrast in a LASER pico-projector using a vibrating symmetric diffuser," *Opt. Express*, vol. 22, no. 6, pp. 6464–6477, 2014.

[22] S. Roelandt, J. Tervo, Y. Meuret, G. Verschaffelt, and H. Thienpont, "Propagation of partially coherent light through a light pipe," *Opt. Express*, vol. 21, no. 14, pp. 17007–17019, 2013.

[23] Q.-L. Deng, B.-S. Lin, P.-J. Wu, K.-Y. Chiu, P.-L. Fan, and C.-Y. Chen, "A hybrid temporal and spatial speckle-suppression method for laser displays," *Opt. Express*, vol. 21, no. 25, pp. 31062–31071, 2013.

[24] M. Sun and Z. Lu, "Speckle suppression with a rotating light pipe," *Opt. Eng.*, vol. 49, no. 2, 2010, Art. no. 024202.

[25] P. Hlubina, "Spectral and dispersion analysis of laser sources and multimode fibres via the statistics of the intensity pattern," *J. Mod. Optic.*, vol. 41, no. 5, pp. 1001–1014, 1994.

[26] B. Saleh and M. Teich, "Reflection and refraction," in *Fundamentals of Photonics*. Hoboken, NJ, USA: Wiley, 2009, pp. 209–215.

[27] Y. Deng and D. Chu, "Coherence properties of different light sources and their effect on the image sharpness and speckle of holographic displays," *Sci. Rep.*, vol. 7, p. 5893, Jul. 2017.

[28] Z. Tong, S. Song, S. Jia, and X. Chen, "Nonsequential speckle reduction method by generating uncorrelated laser subbeams with equivalent intensity using a reflective spatial light modulator," *IEEE Photon. J.*, vol. 9, no. 5, Oct. 2017, Art. no. 7000508.

ZHAOMIN TONG received the Ph.D. degree in electronics and telecommunication from the Norwegian University of Science and Technology, Norway, in 2013. He is currently a Distinguished Professor with the State Key Laboratory of Quantum Optics and Quantum Optics Devices, Institute of Laser Spectroscopy, Shanxi University, China. His research interests include laser projection displays and micro-nano technology.

CHANGYUAN SUN received the B.E. degree from the Nanyang Institute of Technology, China, in 2019. He is currently pursuing the M.E. degree in optical engineering with Shanxi University, China. His current research interest includes laser projection displays.

YIFEI MA received the Ph.D. degree from the Sungkyunkwan University, South Korea, in 2016. He is currently an Assistant Professor with the State Key Laboratory of Quantum Optics and Quantum Optics Devices, Institute of Laser Spectroscopy, Shanxi University, China. His research interest includes synthesis and functionalization of low-dimensional materials and the applications.

MEI WANG received the Ph.D. degree from the Sungkyunkwan University, South Korea, in 2014. She worked as a Postdoctoral Researcher with Sungkyunkwan University, until 2017. She is currently a Professor with the State Key Laboratory of Quantum Optics and Quantum Optics Devices, Institute of Laser Spectroscopy, Shanxi University, China. Her research interests include graphene-based materials, electrophoretic deposition, electrode materials for energy storage devices, and electrochemical sensing.

SUOTANG JIA received the Ph.D. degree from East China Normal University, China, in 1994. From 1997 to 2000, he was the Director of the Department of Electronics and Information Technology, Shanxi University, China. From 2000 to 2010, he was the Vice President of the Shanxi University, and the Director of the Optics Institute of Shanxi. From 2010 to 2012, he was the President of the North University of China. From 2012 to 2018, he was the President of Shanxi University. His research interest includes laser spectroscopy and quantum optics.

XUYUAN CHEN received the Ph.D. degree in semiconductor materials and devices from the Eindhoven University of Technology, The Netherlands, in 1997. Since 1997, he has been with the Physics Department, University of Tromso, Norway, as an Associate Professor, and continued as a Professor, until 2002. Since 2004, he has also been a Professor with the Department of Microsystems, University of South-Eastern Norway, Norway. He has broad experience from national and international collaboration, working groups and organizations. He is author or coauthor of more than 200 scientific publications in international journals and conferences, invited talks and overview articles in the area of semiconductor technology and micro-systems.